PCNA-dependent accumulation of CDKN1A into nuclear foci after ionizing irradiation

Claudia Wiese[2*], Jeanette Heede Rudolph[1], Burkhard Jakob[1], Daniela Fink[1], Frank Tobias[1], Christine Blattner[3] and Gisela Taucher-Scholz[1*]

[1]GSI Helmholzzentrum für Schwerionenforschung, Planckstrasse 1, 64291 Darmstadt, Germany; Tel. +49 6159 712606; Fax. +49 6159 712159.

[2]Lawrence Berkeley National Laboratory, Berkeley, CA 94720, USA; Tel. +1 510 486 4024; Fax. +1 510 486 6816.

[3]Karlsruhe Institute of Technology; Institute of Toxicology and Genetics, PO Box 3640, 76021 Karlsruhe, Germany; Tel. +49 721 60822634; Fax. +49 721 60823354.

*Correspondence: G.Taucher-Scholz@gsi.de, CWiese@lbl.gov

[1]Abbreviations:

[1] LET: linear energy transfer; DSBs: DNA double-strand breaks; SSBs: DNA single-strand breaks; CPD: cumulative population doublings; NHDFs: neonatal human dermal fibroblasts; TLC: thin-layer cellulose; ICQ: Intensity Correlation Quotient; ICA: Image Correlation Analysis.

LBNL/DOE funding & contract number: DE-AC02-05CH11231

DISCLAIMER

DISCLAIMER

This document was prepared as an account of work sponsored by the United States Government. While this document is believed to contain correct information, neither the United States Government nor any agency thereof, nor The Regents of the University of California, nor any of their employees, makes any warranty, express or implied, or assumes any legal responsibility for the accuracy, completeness, or usefulness of any information, apparatus, product, or process disclosed, or represents that its use would not infringe privately owned rights. Reference herein to any specific commercial product, process, or service by its trade name, trademark, manufacturer, or otherwise, does not necessarily constitute or imply its endorsement, recommendation, or favoring by the United States Government or any agency thereof, or The Regents of the University of California. The views and opinions of authors expressed herein do not necessarily state or reflect those of the

1. Introduction

The spatiotemporal coordination of DNA damage repair is crucially important to maintain genomic stability and prevent carcinogenesis. To do so, eukaryotes have evolved a variety of complex DNA repair pathways that are targeted towards a plethora of endogenously and exogenously generated DNA lesions. These DNA repair pathways are tightly interwoven with transcription, apoptosis and cell cycle regulation within a network that is known as the DNA damage response (for review see: [1]. Within this network the cyclin-dependent kinase (CDK) inhibitor CDKN1A (also known as p21/WAF1/CIP1 [2-4]) plays an important role. CDKN1A is involved in growth arrest through cell cycle checkpoints (for review see [5]), in regulating apoptosis [6-11] and gene expression/transcription [12-14], in inhibiting DNA replication by interacting directly with proliferating cell nuclear antigen (PCNA) and CDK complexes [15-18], and in the negative regulation of translesion DNA synthesis (for review see [19, 20]. CDKN1A's pleiotropy is regulated by its expression levels, its sub-cellular localization, its protein binding partners and its phosphorylation status [21, 22].

CDKN1A is a member of the CIP/KIP family of CDK inhibitors, which inhibit cyclin D-, E-, and A-dependent kinase activity [2, 3, 15, 23, 24]. In solution, CDKN1A is an intrinsically unstructured protein [25] presumably allowing it to adopt multiple conformations upon interaction with specific binding partners [26]. At its carboxy terminus (R143-S160), CDKN1A interacts with PCNA, the accessory protein of DNA polymerases δ and ε. Phosphorylation of CDKN1A at T145 leads to loss of the inhibition of DNA replication and to loss of PCNA-binding [27-29], and how the CDKN1A-PCNA interaction can affect DNA damage repair has been a subject of intense investigation (for review see [30]).

We have shown previously that in nuclei of normal human fibroblasts the CDKN1A protein accumulates into foci at highly clustered DNA damage sites within minutes after traversal by accelerated charged particles [31, 32]. CDKN1A foci formation is independent of functional TP53, NBS and ATM [31, 33], and a strict spatial correlation for the signals of CDKN1A and MRE11, γH2AX and PCNA was observed at the sites of

---

particle traversal [34]. However, it must be considered that DNA damage induced by high linear energy (LET) charged particle irradiation, besides predominantly DNA double-strand breaks (DSBs), likely additionally contains in close proximity multiple other lesions, including damaged DNA bases and DNA single-strand breaks (SSBs) [35]. We now show that CDKN1A also accumulates into foci after exposure to X-rays, and after treatment with H_2O_2. We provide evidence that recruitment of CDKN1A after radiation damage is dependent on its direct interaction with PCNA. Furthermore, live-cell imaging analysis of ectopically expressed EGFP-CDKN1A and dsRED-PCNA reveals that PCNA is recruited with slightly faster kinetics. Interestingly, recruitment of CDKN1A after radiation damage in nucleotide excision repair-deficient XPA cells is not different from wild type cells. These results support the notion that CDKN1A accumulation into foci in response to ionizing radiation is distinct from its role in nucleotide excision repair. We suggest that the local recruitment of CDKN1A by PCNA to DNA lesions induced by ionizing radiation or H_2O_2 is unrelated to DSB repair and serves to regulate the multiple protein interactions of PCNA required for faithful and efficient long-patch base excision repair.

2. Material and methods

2.1. Cell culture, transfection, CDKN1A expression plasmids and immunoprecipitations

Confluent normal human foreskin fibroblasts (AG1522C, Coriell Cell Repository, passage number 8-15, cumulative population doublings (CPD) 20-30), neonatal human dermal fibroblasts (NHDFs; CellSystems Biotechnologie, passage number 6-12, CPD 11-20) and XPA-deficient human GM00710B fibroblasts (Coriell Cell Repository, passage number 18-20, CPD 6-10) were grown in EMEM medium (BioWhitaker/Cambrex) with 15% fetal calf serum (FCS; Biochrom), 1% L-glutamine (Biochrom), 0.5% penicillin/streptomycin (Biochrom) at 37°C and a 5% CO_2 atmosphere. Cells were grown 10–14 days with bi-weekly medium changes until confluent and arrested in G_0/G_1-phase. Cell cycle analysis was performed by flow cytometry as described [33] using a PAS III flow cytometer (Partec) to ensure that approximately 85–95% of growth-arrested cells were in G_0/G_1. Parental HCT116 cells and the CDKN1A/p21-deficient HCT116 cells were kindly provided by Dr. B. Vogelstein (Johns Hopkins University, Baltimore) and maintained as described previously [36]. HeLa cells and EM9 cells were maintained as described [37]. HeLa, EM9 and HCT116 cells were

transfected using Lipofectamine2000 (Invitrogen) using standard procedures. Transfection of fibroblasts was done using AMAXA nucleofector (Lonza) according to the manufacturer's protocols.

Wild type and mutant (T145A and T145D) CDKN1A expression plasmids in the pcDNA3.1-*myc*-his_6 vector (Invitrogen) are described elsewhere [27] and were kindly provided by Dr. S. Dimmeler (Goethe University, Frankfurt am Main). EGFP-CDKN1A was generated by amplifying the *CDKN1A* ORF from the wild type CDKN1A expression plasmid [27] and by cloning the amplified *CDKN1A* ORF into pEGFP-C2 (Clontech) from *Hin*dIII to *Xba*I. The PCNA construct was generated as described in [38], but using a DsRed-tag and was kindly provided by Dr. M. Cardoso (Technical University, Darmstadt).

Immunoprecipitations were carried out in RIPA buffer (1% NP40, 50 mM Tris-HCl, 150 mM NaCl, 1 mM EDTA, 0.5% sodium deoxycholate) with protease inhibitor cocktail (Roche) and essentially as described [27], using anti-cMyc rabbit polyclonal antibody (Santa Cruz; A14) or polyconal rabbit anti-CDKN1A (Ab-5 antibody, Oncogene).

2.2. Irradiation and H_2O_2 treatment

For experiments involving peptide mapping the cells were irradiated with γ-rays from a Gammacell 220 irradiator (A.E.C.L. Atomic energy of Canada limited, Ottawa, Canada) with a ^{60}Cobalt source. Cells were irradiated with dose rates of 2 Gy/min at room temperature.

Exposure to X-rays was performed using an industrial X-ray generator (Isovolt DS1, type IV320-13 (Seifert) at 250 kV and 16 mA. This X-ray tube is equipped with a 7 mm beryllium filter and one aluminium and one copper filter of 1 mm thickness each to eliminate soft X-rays. All samples were irradiated at room temperature at dose rates of 2–3.5 Gy/min. Exposure to heavy ions was carried at the UNILAC facility at the Helmholtzzentrum für Schwerionenforschung (Darmstadt) as described previously [31]. All ion species used throughout this study are depicted in Table I.

Table I

UV micropore irradiation was based on the method described previously [39]. The medium was removed, the cells were rinsed twice with PBS and immediately after covered by polycarbonate foils containing pores of 3 μm diameter in size. These filters

were produced in-house by pre-irradiation with charged particles and subsequent etching in NaOH solution for 80 min. Cells covered by polycarbonate filters were irradiated with 100 J/m^2 UV-C light (254 nm) which took about 10 seconds. Following irradiation, polycarbonate filters were removed and immediately filled with warm growth medium.

For H_2O_2 treatment, cell were rinsed with PBS and incubated with 0.2 mM H_2O_2 in PBS for 20 min at room temperature. H_2O_2 was removed, cells were washed several times in warm PBS and then incubated at 37°C for 15 min in regular growth medium before fixation.

2.3. Immunofluorescence assay

Cells were fixed in 4% paraformaldehyde and immunostained as described previously [31]. For CDKN1A detection, cells were permeabilized in Hepes buffer before fixation as described [33]. PCNA immunostaining was performed as described in [34] using cytoskeleton buffer for pre-extraction. The following primary antibodies were used: mouse anti CIP1/WAF1 (BD; dilution 1:80); mouse anti PCNA (Chemicon; 1:50); mouse/rabbit anti γH2AXser139 (Millipore; 1:500); mouse/rabbit anti 53BP1 (Bethyl Laboratories; 1:2000) and rabbit anti XRCC1 (Alexis Biochemicals; 1:1000). Alexa 488 goat anti-mouse IgG F(ab')2 and Alexa 568 goat anti-mouse IgG F(ab')2 (Molecular Probes) were used at 5 μg/ml. DNA was stained with 1 μM ToPro-3 (Molecular Probes). The samples were air-dried and mounted in Vectashield solution (Vector Laboratories).

2.4. Phosphopeptide mapping

HeLa cells grown in phosphate-free growth medium with 10% dialyzed FCS (Biochrom) were transfected with the wild type CDKN1A expression construct 24 h prior to mock irradiation or exposure to 10 Gy γ-rays. Immediately following irradiation, 2.5 mCi [32P]-orthophosphate was added to each 15-cm dish and incubated for 2.5 h at 37°C before cells were lysed on ice in NP40 lysis buffer (10 mM NaH2PO4 pH 7.0, 1% NP40, 50 mM Tris-HCl, pH 8.0, 5 mM EDTA, 150 mM NaCl and 1 mM AEBSF). The lysates were cleared by centrifugation and supernatants were collected for anti-CDKN1A immunoprecipitation as described in section 2.5. Immunoprecipitated complexes were separated on 10% SDS-PAGE gels using standard procedures. The gels were dried and exposed to Hyperfilm MP (GE Healthcare) overnight. Bands containing ectopic CDKN1A-*myc*-his$_6$ were excised from the gel and were mashed using a Kontes tissue

grinder, and 500 μl 50 mM NH_4HCO_3, pH 7.4, 10 μl 20% SDS solution and 10 μl β-mercaptoethanol were added before the samples were boiled for 5 min. To extract protein from gel the suspension was incubated on a rocker for at least 4 h at room temperature. The gel slurry was separated from the supernatant by centrifugation. The first elution was repeated and both cleared eluates were combined, placed on ice for cooling and 20 μg RNase carrier protein and 250 μl ice-cold TCA were added for protein precipitation. Precipitates were collected by microcentrifugation and washed in 500 μl ice-cold 95 % ethanol. The protein pellets were then air-dried and resuspended in 50 μl freshly prepared and ice-cold performic acid for 60 min on ice. 400 μl H_2O were added, the samples were frozen on dry ice and the performic acid was evaporated under vacuum in a SpeedVac evaporator. For proteolytic digestion, protein pellets were resuspended in 50 μl 50 mM NH_4HCO_3, pH 8.0, 10 μg trypsin was added and digests were carried out at 37°C overnight. 10 μg of fresh trypsin was added and incubated for further 4 h. Four times 400 μl H_2O were added individually and samples were lyophilized after each step using a SpeedVac evaporator. The tryptic digests then were resuspended in 400 μl electrophoresis buffer (7.8 % formic acid, 2.5 % glacial acetic acid) pH 1.9, the peptide solutions were cleared by microcentrifugation, and the supernatants were lyophilized. Digests were resuspended in 5 μl pH 1.9 electrophoresis buffer and each sample was spotted onto thin-layer cellulose (TLC) plates for first-dimension electrophoresis at 500 V for 1.5 h. Before second-dimension chromatography, TLC plates were air-dried and then placed for 6 h in phosphopeptide chromatography buffer (37.5 % n-butanol, 25 % pyridine, 7.5 % glacial acetic acid), after which TLC plates were dried again and exposed to Hyperfilm MP for 3-4 weeks.

2.5. Cell fractionation and western blot analysis

For sub-nuclear cell fractionation cells were rinsed in ice-cold PBS, trypsinized and resuspended at 10^7 cells/ml in hypotonic lysis buffer (10 mM Tris-HCl pH 7.4, 2.5 mM $MgCl_2$, 0.5% NP40, 1 mM DTT, 1 mM AEBSF and protease inhibitors). Cells were lysed on ice for 10 min as described previously [40]. To separate soluble proteins from the chromatin-bound protein fraction, the suspension was centrifuged at 300 × g for 1 min. The pellet containing the chromatin-bound proteins and cell debris was washed twice in wash buffer (10 mM Tris-HCl pH 7.4, 150 mM NaCl, 1 mM AEBSF, and protease inhibitors) and re-pelleted at 300 × g for 1 min. The pellet was resuspended in

DNase I solution (10^8 cells/ml; 20 mM NaCl, 0.1 mM AEBSF and 200 units Benzonase / 10^7 cells). Benzonase digests were carried out for 45 min at 4°C. After centrifugation at 14000 × g for 1 min (4°C) chromatin-bound protein fractions (supernatant) were separated from pellets and pellets were resuspended in 70 µl 2 X Laemmli buffer [41] for Western blot analyses according to our standard procedures [42]. The following primary antibodies were used: mouse anti CIP1/WAF1 (BD; 1:4000) and rabbit anti CDK2 (BD; 1:1000); mouse anti PCNA (Chemicon; 1:4000); rabbit anti β-actin (Sigma; 1:5000) and mouse anti α-tubulin (Sigma; 1:5000).

2.6. Microscopy

Microscopic analysis of fixed samples was carried out on a confocal microscope as described previously [31, 34]. A Leica TCS confocal laser scanning system equipped with a DM IRBE inverted microscope (lens: Plan Apo 63× / 1.32 oil) and an argon/krypton laser were used.

2.7. Live-cell imaging

Measurements of recruitment kinetics were essentially done as described [37]. Time-lapse series during and after irradiation was recorded using a remote controlled EB-CCD (Hamamatsu C7190-53) mounted on an Olympus IX71 microscope equipped with a 60× water immersion NA1.2 Plan Apo lens. To describe the dynamics of CDKN1A and PCNA after irradiation with charged particles, the following simplified sequential binding model was used:

$$[PCNA] + [D] \xrightarrow{k1} [PCNA\text{-}D] \qquad [PCNA\text{-}D] + [CDKN1A] \xrightarrow{k2} [CDKN1A\text{-}PCNA\text{-}D]$$

with D describing the concentration of damage sites, and [PCNA] and [CDKN1A] corresponding to free PCNA and CDKN1A, respectively. [PCNA-D] is PCNA bound to damaged DNA and [CDKN1A-PCNA-D] indicates the additional binding of CDKN1A. Assuming that the concentrations of the proteins are not limiting, with [PCNA] >> [D] and [CDKN1A]>>[PCNA-D], the equation can be simplified to pseudo first order kinetics, leading to the following equations describing the mono-exponential accumulation of PCNA

(1) $[PCNA\text{-}D] = [D_0] \times (1-\exp(-t \times k1^*))$,

and the biphasic fitting equation for the recruitment of CDKN1A

$$(2)\qquad [\text{CDKN1A-PCNA-D}] = [D_0] \times \frac{(1-\exp(-t \times k2^*))k1^* + (1-\exp(-t \times k1^*))k2^*}{k1^* - k2^*}$$

in which $[D_0]$ is the concentration of initially damaged DNA sites and t refers to the time in seconds. For the fitting procedure of CDKN1A binding, k1* resulting from the fitting of (1) to the PCNA data was used as an input into the equation and only k2* was treated as free parameter.

2.8. Image analysis

Maximum projections of confocal image stacks were performed using ImageJ. The "Image Correlation Analysis" plugin (Dr. J. Balaji, Department of Neurobiology, UCLA) of the MBF ImageJ bundle was used for colocalization analysis as previously described [43] yielding Intensity Correlation Quotient (ICQ) values between -0.5 and +0.5 indicating random staining (ICQ~0) segregated staining ($0 > ICQ \gtrsim -0.5$) or dependent staining ($0 < ICQ \leq +0.5$). The analysis of the recruitment kinetics was done using the Time Series Analyzer plugin of ImageJ as described in [37].

3. Results

3.1. CDKN1A foci are induced by X-irradiation and do not co-localize with DSB markers

Confluent growth arrested AG1522C cells were exposed to 10 Gy X-rays and analyzed for nuclear accumulations of both CDKN1A and γH2AX. As shown in Fig. 1A, distinct accumulations of CDKN1A were detected in some nuclei of X-irradiated cells as early as 1 h post exposure. CDKN1A foci were most pronounced at 3 h and remained present until 5 h post irradiation. After 22 h, none of the irradiated nuclei displayed CDKN1A foci whereas a fraction of irradiated cells still showed γH2AX foci. In addition, at any given time-point analyzed, X-ray-induced CDKN1A and γH2AX foci did not co-localize (see below).

To test whether the accumulation of CDKN1A into foci is dose-dependent, growth arrested AG1522C fibroblasts were irradiated with 2, 4, 6, or 8 Gy X-rays and fixed at 3 h post irradiation, at which time most of the DSBs induced by X-irradiation are expected to be repaired [44]. Compared to control cells, cells exposed to 2 Gy X-rays

showed very few and very small radiation-induced CDKN1A foci and some γH2AX foci (Fig. 1B). However, with an increase in X-ray dose the number and the distinctiveness of CDKN1A foci increased, as did the number of γH2AX foci. For each X-ray dose tested, the number of induced CDKN1A foci was noticeably higher than the number of γH2AX foci. Using image correlation analysis (ICA), these X-ray-induced CDKN1A and γH2AX foci were determined as not colocalizing, yielding an intensity correlation quotient (ICQ) of 0.036 (Fig. 1C; panel a for the nucleus shown on the right). This value around 0 is indicative of random staining (see materials and methods) strongly suggesting that CDKN1A is not accumulating at the sites of DSBs. After exposure to increasing doses of X-rays, the same pattern of non-overlapping foci was observed for CDKN1A and 53BP1, another known DSB marker (suppl. Figs. 1A and 1B), also suggesting that CDKN1A accumulation into foci in response to X-rays is independent of DNA DSB formation.

An early recruitment of CDKN1A into foci and their colocalization with PCNA has been described in nucleotide excision repair (NER) [45]. In addition, we previously reported on the colocalization of CDKN1A and PCNA foci at the sites of charged particle traversal [34]. To test whether CDKN1A and PCNA foci would colocalize in response to low LET ionizing radiation (IR), we exposed G0/G1 AG1522C fibroblasts to 8 Gy X-rays and fixed and stained nuclei for both CDKN1A and PCNA, as previously described (BJ, RR, 2003). As described above, CDKN1A foci are readily observable at 3 h after 8 Gy X-rays (Fig. 1D, panel a), as are PCNA foci (Fig. 1D, panel b). In addition, PCNA and CDKN1A foci frequently are colocalizing (Fig. 1D, panels c-d). The ICQ of 0.181 and in particular the shapes of the ICA plots are in strong support of a colocalization between PCNA and CDKN1A after X-irradiation (Fig. 1D, panel e). As previously for CDKN1A and γH2AX, we also tested for the colocalization between PCNA and γH2AX. In response to 8 Gy X-rays, we find no colocalization of PCNA and γH2AX (suppl. Figs. 1C and 1D).

3.2. CDKN1A forms foci in response to H_2O_2 treatment

Next we tested whether CDKN1A would be recruited into foci after treatment with H_2O_2. NHDFs were treated in 0.2 mM H_2O_2 for 15 min and fixed and stained after an additional 15 min in regular growth medium at 37°C. Fig. 2A shows a representative NHDF nucleus after treatment with H_2O_2 in which both XRCC1 (panel f) and CDKN1A (panel g) were recruited into foci. Individual NHDF nuclei were tested for colocalization of CDKN1A and XRCC1 using ICA, as exemplarily depicted for one H_2O_2-exposed nucleus in Fig. 2B. The only slightly positive mean ICQ value of 0.111 obtained from the

analysis of 10 different nuclei suggests that CDKN1A and XRCC1 apparently are not clearly colocalizing, but also are not anti-correlated, pointing to their partial random overlap. To exclude the possibility that H_2O_2-treatment could lead to structural changes within the chromatin that may impair CDKN1A and/or XRCC1 recruitment, NHDFs were treated with 0.2 mM H_2O_2 for 15 min first and subsequently irradiated with nickel ions. As observed for nickel ion exposure only (data not shown), treatment of NHDFs with 0.2 mM H_2O_2 followed by nickel ion exposure led to CDKN1A and XRCC1 foci that co-localized (suppl. Fig. 2A), indicating that H_2O_2 treatment does not impair the recruitment of CDKN1A and of XRCC1 to the sites of charged particle-induced highly clustered radiation damage. Taken together, these results show that CDKN1A and XRCC1 are recruited into focal structures after H_2O_2 treatment, but without strong evidence for their colocalization after X-irradiation. Similarly to CDKN1A and XRCC1 which colocalized after charged particle exposure (suppl. Fig. 2A), CDKN1A and 53BP1 also colocalized in the tracks of heavy ion traversals (suppl. Fig. 2B). Of note, ectopically expressed human CDKN1A formed foci in XRCC1-deficient EM9 hamster cells irradiated with heavy ions (suppl. Fig. 2C), suggesting that CDKN1A recruitment in response to radiation damage is independent of XRCC1.

3.3. CDKN1A foci formation after ionizing radiation is not delayed in XPA cells

To further investigate the role of CDKN1A recruitment to DNA damaged sites, we compared nucleotide excision repair (NER)-proficient AG1522C cells and NER-deficient XPA (Xeroderma Pigmentosum complementation group A) cells exposed to 100 J/cm^2 UV-light under a microfilter-mask, carried out essentially as described before [39]. Recruitment of both PCNA and CDKN1A was detected in AG1522C nuclei at 30 min and 5 h after exposure to UV-C light (Fig. 3A, panels a & b and e & f, respectively). In contrast, NER-deficient XPA cells show no accumulation of either PCNA or CDKN1A to the sites of UV-C-induced DNA damage at 30 min after exposure (Fig. 3A, panels c and g, respectively), but do show delayed accumulation of both proteins into foci (Fig. 3A, panels d and h), in accord with previous observations [45]. Next, AG1522C and XPA cells were exposed to argon ions. In AG1522C cells, PCNA and CDKN1A were detected as distinct foci at 30 min post exposure (Fig. 3B, panels a and e) and at 5 h post exposure (Fig. 3B, panels b and f, respectively), very similar to the response observed after UV-C light. In addition, in XPA cells recruitment of both PCNA and CDKN1A occurred early (*i.e*. within 30 min) after argon ions (Fig. 3B, panels c and g, respectively)

and in contrast to what we observed after UV-C microfilter-mask irradiation. These results strongly suggest a role for CDKN1A recruitment in a DNA repair pathway different from NER.

3.4. CDKN1A foci formation in response to ionizing radiation is dependent on PCNA

As shown in Fig. 3B and as reported previously [33], CDKN1A and PCNA localize at heavy ion-induced DNA lesions. Previously, however, we had not tested for a direct interaction of CDKN1A and PCNA when recruited in response to charged particle radiation. Here, we have tested whether recruitment of CDKN1A after exposure to heavy ions is dependent on its physical interaction with PCNA. To do so, we have used three different expression constructs for C-terminally *myc*-his_6-tagged CDKN1A (wild type, phosphomimetic (T145D) and non-phosphorylatable (T145A)) as described by Roessig *et al*. [27]. We assessed CDKN1A recruitment of ectopically expressed CDKN1A after charged particle irradiation in transiently transfected HCT116 cells deficient for the endogenous *CDKN1A* gene [36], and in HeLa cells that express very low levels of endogenous CDKN1A. Representative Western blots to show the expression of the wild type and mutant versions of CDKN1A in CDKN1A-deficient HCT116 cells and in HeLa cells are depicted in suppl. Fig. 3A and 3B. To test for the interaction between ectopically expressed CDKN1A and PCNA, anti-CDKN1A immunoprecipitations were carried out using HeLa cells lysates with ectopically expressed wild type and mutant versions of CDKN1A. PCNA was precipitated in anti-CDKN1A complexes from HeLa cells expressing wild type CDKN1A or CDKN1A-T145A, but not from HeLa cells expressing CDKN1A-T145D (Fig. 4A). We also monitored the presence of CDK2 in anti-*myc* complexes from HeLa cells ectopically expressing wild type CDKN1A, CDKN1A-T145D or CDKN1A-T145A. Compared to wild type CDKN1A, CDK2 was present in reduced amounts in anti-*myc* complexes from HeLa cells expressing CDKN1A-T145D (suppl. Fig. 3C), as reported previously for expression of the same wild type and mutant versions of CDKN1A in COS-7 cells [27].

Next, we asked whether ectopically expressed wild type and mutant CDKN1A would relocalize into foci in response to charged particle irradiation. HeLa cells and HeLa cells transfected with the one of the three CDKN1A expression constructs were irradiated with accelerated heavy ions and tested for CDKN1A foci formation by immunostaining. Untransfected HeLa cells, mock irradiated or after exposure to zinc ions, did not form CDKN1A foci (Fig. 4B, panels a and b) whereas irradiated HeLa cells transfected to

express wild type CDKN1A or CDKN1A-T145A did (Fig. 4B, panels d and f, respectively). In contrast, HeLa cells transfected to express the phosphomimetic version of CDKN1A (CDKN1A-T145D) did not show CDKN1A foci after irradiation with gold ions (Fig. 4, panel h). Instead, CDKN1A-T145D remained homogeneously distributed throughout the nuclei without relocalizing into foci in response to charged particle irradiation. When CDKN1A-T145D was ectopically overexpressed in CDKN1A-deficient HCT116 cells, essentially the same results were obtained (suppl. Fig. 4). These data show that the direct physical interaction between CDKN1A and PCNA is required for the recruitment of CDKN1A into foci in response to radiation damage.

3.5. CDKN1A is de-phosphorylated after γ-irradiation

To form radiation-induced foci CDKN1A requires the interaction with PCNA. For the CDKN1A-PCNA interaction to occur, CDKN1A has to be dephosphorylated as demonstrated here directly in HeLa cells by immunoprecipitation (Fig. 4A), and also by a very similar analysis earlier in COS-7 cells [27]. Next, we used peptide mapping to test for the radiation-induced dephosphorylation of CDKN1A in transfected HeLa cells that expressed wild type CDKN1A-*myc*-his_6 transiently. Fig. 5A displays the autoradiograph obtained after first-dimension electrophoresis of anti-CDKN1A complexes from ^{32}P orthophosphate-labeled mock-irradiated HeLa cells and HeLa cells exposed to 10 Gy γ-rays. Second-dimension chromatography shows that the expression of CDKN1A phospho-peptides is abundant in mock-irradiated HeLa cells (Fig. 5B, upper panel). However, no signals for CDKN1A phospho-peptides were detected in anti-CDKN1A complexes from CDKN1A-*myc*-his_6 expressing HeLa cells 2.5 h after exposure to 10 Gy γ-rays (Fig. 5B, lower panel). These results clearly demonstrate that γ-irradiation leads to the dephosphorylation of CDKN1A, and are in accord with our data presented in Fig. 4, in which we show that phosphomimetic CDKN1A-T145D that is unable to directly interact with PCNA also is unable to re-localize into foci after charged particle irradiation.

3.6. CDKN1A and PCNA are part of a chromatin-bound protein fraction after X-irradiation

We used fractionated extracts to test if both CDKN1A and PCNA would localize to the chromatin fraction in response to ionizing radiation. Quiescent AG1522C cells were irradiated with 8 Gy or 30 Gy X-rays and subjected to sub-cellular fractionation 3 h post exposure. As determined by western blot analysis, PCNA was not detected in the

chromatin fraction in control cells that were not exposed to X-rays (Fig. 5C, lane 4). However, a significant amount of PCNA is detected in the chromatin fraction 3 h after exposure to 8 Gy or 30 Gy X-rays (Fig. 5C, lanes 5 and 6, respectively). In several independent experiments we also observed that the association of PCNA with the chromatin fraction in response to X-rays is dose-dependent (compare signal intensities for PCNA in Fig. 5C, lanes 5 and 6). Independent of the radiation dose applied, no PCNA was detected in the pellet remaining after benzonase digest (Fig. 5C, lanes 7-9).

Next we tested whether the incubation time after X-ray exposure would affect the fraction of PCNA associated with the chromatin. To do so, we exposed quiescent AG1522C cells to 30 Gy X-rays and subjected these cells to sub-cellular fractionation at 1 h and 3 h post exposure (Fig. 5D). As before, PCNA was not present in the chromatin fraction of quiescent AG1522C cells not exposed to X-rays (Fig. 5D, lane 4). However, PCNA was detected in the chromatin fraction of irradiated cells analyzed at 1 h or 3 h after X-ray exposure (Fig. 5D, lanes 5 and 6). In addition, while soluble CDKN1A was detected in control and in irradiated samples (Fig. 5D, lanes 1 and 2-3, respectively), CDKN1A was undetectable in the chromatin fraction of unirradiated cells (Fig. 5D, lane 4). However, 1 h after exposure to 30 Gy X-rays a small amount of CDKN1A, and at 3 h post exposure a distinct amount of CDKN1A was associated with the chromatin fraction (Fig. 5D, lanes 5 and 6, respectively). Similarly, at 1 h after exposure to chrominum ions, the fraction of chromatin-bound PCNA was greatly enhanced compared to mock-irradiated cells (Fig. 5E, lane 6). In addition, CDKN1A was also associated with the chromatin after chromium ion exposure (Fig. 5E, lane 6). Taken together, these results show that both PCNA and CDKN1A become components of the chromatin-associated protein fraction in response to low and high LET ionizing radiation.

3.7. Spatiotemporal dynamics of EGFP-CDKN1A and dsRed-PCNA recruitment to radiation damage

To directly measure the dynamical behavior of CDKN1A in comparison to that of PCNA, we analyzed the recruitment kinetics of EGFP-CDKN1A (see Methods) and of dsRed-tagged PCNA [38] to ion-induced DNA damage sites in living cells. For this purpose, both proteins were ectopically expressed in HeLa cells and the formation of foci at damaged sites was observed directly during charged particle irradiation using live-cell imaging microscopy, as described previously [37]. The dynamics of the EGFP-CDKN1A and dsRed-PCNA signals at the sites of uranium ion traversals is depicted in Fig. 6A.

Both proteins started to accumulate within seconds after ion impact reaching maximum fluorescence intensities about 7 min post irradiation. Compared to dsRed-PCNA, EGFP-CDKN1A appeared with a slight delay. While a mono-exponential curve fitting with a time constant of 108 +/- 5 s (confidence interval) well described the kinetics of PCNA binding to sites of damage, a single exponential model clearly did not fit the sigmoid shape of the experimental data for CDKN1A recruitment, suggesting that binding of CDKN1A is not the primary process. The association of EGFP-CDKN1A to damaged sites was best described according to a bi-exponential kinetics based on the preceding binding of PCNA. Based on the time constant of 108 s determined for PCNA which is required to generate CDKN1A binding sites, a secondary time constant of 92 +/- 4 s was calculated for the CDKN1A association step.

In order to confirm that the recruitment of CDKN1A to DNA damage sites occurred independently of NER, we further compared the relocation of EGFP-CDKN1A in wild type (AG1522C) and XPA deficient human GM00710B fibroblasts using high time resolution live-cell imaging. After irradiation with xenon ions, ectopically expressed EGFP-CDKN1A showed similar spatiotemporal recruitment in both NER-defective and in wild type cells (Fig. 6B; secondary time constants were 131 +/- 4 s and 143 +/- 6 s, respectively). These results indicate a possibly slightly slower dynamics in primary fibroblasts compared to the HeLa tumor cells (see above), and further confirm that binding of CDKN1A to DNA damage sites after ionizing radiation is not related to ongoing NER processes.

4. Discussion

CDKN1A is a cyclin-dependent kinase inhibitor crucially important for the response of cells to genotoxic agents and a major transcriptional target of TP53 [2]. Independent of TP53 transactivation, CDKN1A is recruited to the sites of DNA damage induced by charged particle traversals, as reported by us previously [31, 33]. Meanwhile, an increasing number of studies report that CDKN1A accumulates into focal structures at localized areas of DNA damage (for review see [30]), pointing towards a more direct role for CDKN1A in DNA damage repair.

Our findings described here, for the first time, show that CDKN1A is rapidly recruited to DNA damage sites induced by low LET IR in human cells. We find that the

accumulation of CDKN1A into foci after X-rays is both dose- and time- dependent. We provide evidence that X-ray-induced CDKN1A foci are spatially distinct from the accumulated DSB markers γH2AX and 53BP1. These results lead us to conclude that the accumulation of CDKN1A into foci in response to radiation damage is independent of DNA DSB repair. In prior studies, we consistently observed the colocalization of CDKN1A and DSB markers, such as 53BPı (see suppl. Fig. 2B) and MRE11/RAD50 [33], at local sites of highly clustered radiation damage. This can be explained by the production of different types of lesions in close proximity within the trajectories of heavy ions, confirming the observations of others [35]. Our new data are in accord with a published report in which CDKN1A showed no protection from the cytotoxic effects of X-rays in cell survival assays or in facilitating DSB repair [46]. Taken together, these results and ours strongly argue that CDKN1A recruitment is involved in the response to radiation-induced DNA lesions that are not DSBs.

Furthermore, we provide evidence that both CDKN1A and PCNA foci colocalize in human fibroblasts expose to X-rays. In addition, taking advantage of the production of discrete DNA damage sites and high lesion density using high LET IR, we find that the accumulation of CDKN1A into foci is dependent on its direct interaction with PCNA. This direct interaction with PCNA is facilitated by CDKN1A in its non-phosphorylated state only. In strong support of these findings, we observe that ectopically expressed wild type CDKN1A in HeLa cells undergoes dephosphorylation in response to high doses of low LET γ-irradiation, and that both CDKN1A and PCNA are associated with the chromatin fraction after exposure to high doses of low LET X-rays or high LET chromium ions. Interestingly, CDKN1A dephosphorylation and localization to the chromatin after low LET X-rays occurs within 2-3 h after irradiation, within which time we also find the recruitment of CDKN1A into foci to be most prevalent after X-irradiation.

While this manuscript was in preparation, Koike and collaborators reported the accumulation of CDKN1A at local sites of damaged DNA introduced by UV-A laser irradiation [47]. Similar to our experiments, these investigators describe the inability of ectopically expressed truncated CDKN1A that is unable to interact with PCNA, to accumulate into foci after UV-A laser irradiation. While Koike and collaborators did not use presensitizers, they used a 405-nm laser with a high likelihood for also introducing NER-relevant DNA lesions, as previously discussed [45, 48]. Both laser microirradiation systems and charged particles induce highly localized DNA damage. However, the results obtained with these two different radiation modalities are very difficult to

compare, since, unlike the radiation dose from heavy ions, the delivered laser dose cannot be measured directly, as reported by us in a prior study [49]. Importantly, differences in the DNA damage spectra and the extremely high local dose from UV-A microlasers can lead to the recruitment of specific DNA-binding proteins and repair factors, which, after densely ionizing charged particle irradiation, do not localize to the sites of particle traversal [48, 49]. In addition, while Koike and collaborators [47], in line with our results for high LET radiation, show that rapidly recruited EGFP-CDKN1A co-localizes with a DSB marker after UV-A laser irradiation, our new results in the present study clearly delineate that this is not the case after sparsely ionizing X-irradiation.

Similarly to what has been reported for CDKN1A and PCNA in NER-related processes and for the spatiotemporal dynamics of CDKN1A recruitment to DNA damage sites induced by UV-light [45], we find that CDKN1A recruitment follows PCNA recruitment with slight delay also after charged particle irradiation. Notably, while in XPA-deficient human fibroblasts the recruitment of CDKN1A to local areas of DNA damage sites induced by UV-light is greatly impaired ([45], and this study), we show that in NER-defective XPA-deficient fibroblasts exposed to heavy charged particles CDKN1A recruitment into foci is not different from NER-proficient wild type cells. These results show that binding of CDKN1A to DNA damage sites after ionizing radiation is unrelated to NER processes.

Recently a role for CDKN1A recruitment in base excision repair (BER) challenged by an alkylating agent has been reported [50]. However, after H_2O_2 treatment, we observed only random colocalization between XRCC1 and CDKN1A, arguing that CDKN1A and XRCC1 may function at distinctively different stages of XRCC1-mediated single nucleotide base excision repair (SN-BER) or that the detection of the colocalizing XRCC1 and CDKN1A is experimentally difficult using immunocytohistochemistry. Alternatively, CDKN1A may not be involved in any stage of SN-BER after oxidative DNA damage.

Given the fact that our results for radiation damage which also produces a high number of oxidative DNA lesions show that CDKN1A recruitment is facilitated by PCNA, we favor a model in which CDKN1A via its direct interaction with PCNA responds to IR-induced lesions by BER. It is reasonable to assume that these lesions most likely are repaired by long-patch BER (LP-BER), in which CDKN1A could orchestrate the multiple protein interactions of PCNA that are necessary to faithfully and efficiently conduct this pathway ([30] and references therein). In this regard it is interesting to note that

CDKN1A has been shown to affect LP-BER by inhibiting the PCNA-directed stimulation of FEN-1, DNA ligase I, and DNA polymerase δ [51]. It is also interesting that the interaction of chromatin-bound CDKN1A with PARP-1, that is required for BER following treatment with alkylating agents [50], is independent of PCNA [52]. Taken together, these results and ours suggest that, independent of TP53, through its spatio-temporal recruitment to various chromatin-associated factors of DNA damage repair CDKN1A may regulate the different sub-pathways of BER.

Conflict of interest

The authors declare no conflict of interest.

Acknowledgements

The authors greatly acknowledge technical help by Gudrun Becher, Wolfgang Becher, Günther Lenz and Katja Kratz. This work was supported by Bundesministerium für Bildung und Forschung [02NUK001A] and grant NNJ055HI36I from the National Aeronautics and Space Administration.

References

[1] D. Branzei, M. Foiani, Regulation of DNA repair throughout the cell cycle, Nature reviews, 9 (2008) 297-308.

[2] W.S. el-Deiry, T. Tokino, V.E. Velculescu, D.B. Levy, R. Parsons, J.M. Trent, D. Lin, W.E. Mercer, K.W. Kinzler, B. Vogelstein, WAF1, a potential mediator of p53 tumor suppression, Cell, 75 (1993) 817-825.

[3] J.W. Harper, G.R. Adami, N. Wei, K. Keyomarsi, S.J. Elledge, The p21 Cdk-interacting protein Cip1 is a potent inhibitor of G1 cyclin-dependent kinases, Cell, 75 (1993) 805-816.

[4] A. Noda, Y. Ning, S.F. Venable, O.M. Pereira-Smith, J.R. Smith, Cloning of senescent cell-derived inhibitors of DNA synthesis using an expression screen, Experimental cell research, 211 (1994) 90-98.

[5] G.P. Dotto, p21(WAF1/Cip1): more than a break to the cell cycle?, Biochimica et biophysica acta, 1471 (2000) M43-56.

[6] A. Suzuki, Y. Tsutomi, K. Akahane, T. Araki, M. Miura, Resistance to Fas-mediated apoptosis: activation of caspase 3 is regulated by cell cycle regulator p21WAF1 and IAP gene family ILP, Oncogene, 17 (1998) 931-939.

[7] A. Suzuki, Y. Tsutomi, M. Miura, K. Akahane, Caspase 3 inactivation to suppress Fas-mediated apoptosis: identification of binding domain with p21 and ILP and inactivation machinery by p21, Oncogene, 18 (1999) 1239-1244.

[8] M. Asada, T. Yamada, H. Ichijo, D. Delia, K. Miyazono, K. Fukumuro, S. Mizutani, Apoptosis inhibitory activity of cytoplasmic p21(Cip1/WAF1) in monocytic differentiation, The EMBO journal, 18 (1999) 1223-1234.

[9] H. Schepers, M. Geugien, B.J. Eggen, E. Vellenga, Constitutive cytoplasmic localization of p21(Waf1/Cip1) affects the apoptotic process in monocytic leukaemia, Leukemia, 17 (2003) 2113-2121.

[10] S. Huang, L. Shu, M.B. Dilling, J. Easton, F.C. Harwood, H. Ichijo, P.J. Houghton, Sustained activation of the JNK cascade and rapamycin-induced apoptosis are suppressed by p53/p21(Cip1), Molecular cell, 11 (2003) 1491-1501.

[11] A. Suzuki, H. Kawano, M. Hayashida, Y. Hayasaki, Y. Tsutomi, K. Akahane, Procaspase 3/p21 complex formation to resist fas-mediated cell death is initiated as a result of the phosphorylation of p21 by protein kinase A, Cell death and differentiation, 7 (2000) 721-728.

[12] N.D. Perkins, Not just a CDK inhibitor: regulation of transcription by p21(WAF1/CIP1/SDI1), Cell cycle (Georgetown, Tex, 1 (2002) 39-41.

[13] M.V. Blagosklonny, Are p27 and p21 cytoplasmic oncoproteins?, Cell cycle (Georgetown, Tex, 1 (2002) 391-393.

[14] O. Coqueret, New roles for p21 and p27 cell-cycle inhibitors: a function for each cell compartment?, Trends in cell biology, 13 (2003) 65-70.

[15] Y. Xiong, G.J. Hannon, H. Zhang, D. Casso, R. Kobayashi, D. Beach, p21 is a universal inhibitor of cyclin kinases, Nature, 366 (1993) 701-704.

[16] H. Flores-Rozas, Z. Kelman, F.B. Dean, Z.Q. Pan, J.W. Harper, S.J. Elledge, M. O'Donnell, J. Hurwitz, Cdk-interacting protein 1 directly binds with proliferating cell nuclear antigen and inhibits DNA replication catalyzed by the DNA polymerase delta holoenzyme, Proceedings of the National Academy of Sciences of the United States of America, 91 (1994) 8655-8659.

[17] S. Waga, G.J. Hannon, D. Beach, B. Stillman, The p21 inhibitor of cyclin-dependent kinases controls DNA replication by interaction with PCNA, Nature, 369 (1994) 574-578.

[18] J.M. Gulbis, Z. Kelman, J. Hurwitz, M. O'Donnell, J. Kuriyan, Structure of the C-terminal region of p21(WAF1/CIP1) complexed with human PCNA, Cell, 87 (1996) 297-306.

[19] Z. Livneh, Keeping mammalian mutation load in check: regulation of the activity of error-prone DNA polymerases by p53 and p21, Cell cycle (Georgetown, Tex, 5 (2006) 1918-1922.

[20] C. Prives, V. Gottifredi, The p21 and PCNA partnership: a new twist for an old plot, Cell cycle (Georgetown, Tex, 7 (2008) 3840-3846.

[21] E.S. Child, D.J. Mann, The intricacies of p21 phosphorylation: protein/protein interactions, subcellular localization and stability, Cell cycle (Georgetown, Tex, 5 (2006) 1313-1319.

[22] J. Cmielova, M. Rezacova, p21(Cip1/Waf1) protein and its function based on a subcellular localization, J Cell Biochem, (2011).

[23] Y. Gu, C.W. Turck, D.O. Morgan, Inhibition of CDK2 activity in vivo by an associated 20K regulatory subunit, Nature, 366 (1993) 707-710.

[24] V. Dulic, W.K. Kaufmann, S.J. Wilson, T.D. Tlsty, E. Lees, J.W. Harper, S.J. Elledge, S.I. Reed, p53-dependent inhibition of cyclin-dependent kinase activities in human fibroblasts during radiation-induced G1 arrest, Cell, 76 (1994) 1013-1023.

[25] R.W. Kriwacki, L. Hengst, L. Tennant, S.I. Reed, P.E. Wright, Structural studies of p21Waf1/Cip1/Sdi1 in the free and Cdk2-bound state: conformational disorder mediates binding diversity, Proceedings of the National Academy of Sciences of the United States of America, 93 (1996) 11504-11509.

[26] C.A. Galea, Y. Wang, S.G. Sivakolundu, R.W. Kriwacki, Regulation of cell division by intrinsically unstructured proteins: intrinsic flexibility, modularity, and signaling conduits, Biochemistry, 47 (2008) 7598-7609.

[27] L. Rossig, A.S. Jadidi, C. Urbich, C. Badorff, A.M. Zeiher, S. Dimmeler, Akt-dependent phosphorylation of p21(Cip1) regulates PCNA binding and proliferation of endothelial cells, Molecular and cellular biology, 21 (2001) 5644-5657.

[28] G. Bornstein, J. Bloom, D. Sitry-Shevah, K. Nakayama, M. Pagano, A. Hershko, Role of the SCFSkp2 ubiquitin ligase in the degradation of p21Cip1 in S phase, The Journal of biological chemistry, 278 (2003) 25752-25757.

[29] V. Gottifredi, K. McKinney, M.V. Poyurovsky, C. Prives, Decreased p21 levels are required for efficient restart of DNA synthesis after S phase block, The Journal of biological chemistry, 279 (2004) 5802-5810.

[30] O. Cazzalini, A.I. Scovassi, M. Savio, L.A. Stivala, E. Prosperi, Multiple roles of the cell cycle inhibitor p21(CDKN1A) in the DNA damage response, Mutat Res, 704 (2010) 12-20.

[31] B. Jakob, M. Scholz, G. Taucher-Scholz, Immediate localized CDKN1A (p21) radiation response after damage produced by heavy-ion tracks, Radiation research, 154 (2000) 398-405.

[32] M. Scholz, B. Jakob, G. Taucher-Scholz, Direct evidence for the spatial correlation between individual particle traversals and localized CDKN1A (p21) response induced by high-LET radiation, Radiation research, 156 (2001) 558-563.

[33] B. Jakob, M. Scholz, G. Taucher-Scholz, Characterization of CDKN1A (p21) binding to sites of heavy-ion-induced damage: colocalization with proteins involved in DNA repair, International journal of radiation biology, 78 (2002) 75-88.

[34] B. Jakob, M. Scholz, G. Taucher-Scholz, Biological imaging of heavy charged-particle tracks, Radiation research, 159 (2003) 676-684.

[35] A. Asaithamby, B. Hu, D.J. Chen, Unrepaired clustered DNA lesions induce chromosome breakage in human cells, Proceedings of the National Academy of Sciences of the United States of America, 108 (2011) 8293-8298.

[36] T. Waldman, K.W. Kinzler, B. Vogelstein, p21 is necessary for the p53-mediated G1 arrest in human cancer cells, Cancer research, 55 (1995) 5187-5190.

[37] B. Jakob, J.H. Rudolph, N. Gueven, M.F. Lavin, G. Taucher-Scholz, Live cell imaging of heavy-ion-induced radiation responses by beamline microscopy, Radiation research, 163 (2005) 681-690.

[38] A. Sporbert, P. Domaing, H. Leonhardt, M.C. Cardoso, PCNA acts as a stationary loading platform for transiently interacting Okazaki fragment maturation proteins, Nucleic acids research, 33 (2005) 3521-3528.

[39] S. Katsumi, N. Kobayashi, K. Imoto, A. Nakagawa, Y. Yamashina, T. Muramatsu, T. Shirai, S. Miyagawa, S. Sugiura, F. Hanaoka, T. Matsunaga, O. Nikaido, T. Mori, In situ visualization of ultraviolet-light-induced DNA damage repair in locally irradiated human fibroblasts, The Journal of investigative dermatology, 117 (2001) 1156-1161.

[40] L.A. Stivala, E. Prosperi, Analysis of p21CDKN1A recruitment to DNA excision repair foci in the UV-induced DNA damage response, Methods Mol Biol, 281 (2004) 73-89.

[41] U.K. Laemmli, Cleavage of structural proteins during the assembly of the head of bacteriophage T4, Nature, 227 (1970) 680-685.

[42] C. Fournier, C. Wiese, G. Taucher-Scholz, Accumulation of the cell cycle regulators TP53 and CDKN1A (p21) in human fibroblasts after exposure to low- and high-LET radiation, Radiation research, 161 (2004) 675-684.

[43] Q. Li, A. Lau, T.J. Morris, L. Guo, C.B. Fordyce, E.F. Stanley, A syntaxin 1, Galpha(o), and N-type calcium channel complex at a presynaptic nerve terminal: analysis by quantitative immunocolocalization, J Neurosci, 24 (2004) 4070-4081.

[44] A. Shibata, S. Conrad, J. Birraux, V. Geuting, O. Barton, A. Ismail, A. Kakarougkas, K. Meek, G. Taucher-Scholz, M. Lobrich, P.A. Jeggo, Factors determining DNA double-strand break repair pathway choice in G2 phase, The EMBO journal, 30 (2011) 1079-1092.

[45] P. Perucca, O. Cazzalini, O. Mortusewicz, D. Necchi, M. Savio, T. Nardo, L.A. Stivala, H. Leonhardt, M.C. Cardoso, E. Prosperi, Spatiotemporal dynamics of p21CDKN1A protein recruitment to DNA-damage sites and interaction with proliferating cell nuclear antigen, Journal of cell science, 119 (2006) 1517-1527.

[46] C. Larsson, C.E. Ng, p21+/+ (CDKN1A+/+) and p21-/- (CDKN1A-/-) human colorectal carcinoma cells display equivalent amounts of thermal radiosensitization, Radiation research, 160 (2003) 205-209.

[47] M. Koike, Y. Yutoku, A. Koike, Accumulation of p21 proteins at DNA damage sites independent of p53 and core NHEJ factors following irradiation, Biochem Biophys Res Commun, 412 (2011) 39-43.

[48] E.S. Williams, J. Stap, J. Essers, B. Ponnaiya, M.S. Luijsterburg, P.M. Krawczyk, R.L. Ullrich, J.A. Aten, S.M. Bailey, DNA double-strand breaks are not sufficient to initiate recruitment of TRF2, Nat Genet, 39 (2007) 696-698; author reply 698-699.

[49] J. Splinter, B. Jakob, M. Lang, K. Yano, J. Engelhardt, S.W. Hell, D.J. Chen, M. Durante, G. Taucher-Scholz, Biological dose estimation of UVA laser microirradiation utilizing charged particle-induced protein foci, Mutagenesis, 25 (2010) 289-297.

[50] O. Cazzalini, F. Dona, M. Savio, M. Tillhon, C. Maccario, P. Perucca, L.A. Stivala, A.I. Scovassi, E. Prosperi, p21CDKN1A participates in base excision repair by regulating the activity of poly(ADP-ribose) polymerase-1, DNA repair, 9 (2010) 627-635.

[51] S. Tom, T.A. Ranalli, V.N. Podust, R.A. Bambara, Regulatory roles of p21 and apurinic/apyrimidinic endonuclease 1 in base excision repair, The Journal of biological chemistry, 276 (2001) 48781-48789.

[52] I. Frouin, G. Maga, M. Denegri, F. Riva, M. Savio, S. Spadari, E. Prosperi, A.I. Scovassi, Human proliferating cell nuclear antigen, poly(ADP-ribose) polymerase-1, and p21waf1/cip1. A dynamic exchange of partners, The Journal of biological chemistry, 278 (2003) 39265-39268.

Figure Legends

Figure 1. CDKN1A focus formation in G0/G1 normal human fibroblasts (AG1522C) after X-irradiation. (A) Time course of CDKN1A (green) and γH2AX (red) focus formation after 10 Gy X-rays. (B) CDKN1A (green) and γH2AX (red) focus formation 3 h after exposure to increasing doses of X-rays. (C) Exemplary colocalization analysis for CDKN1A and γH2AX (panel a) for the nucleus shown on the right. Depicted are the ICA (intensity correlation analysis) plots for the proteins as indicated and the respective nucleus stained for CDKN1A (green) and γH2AX (red). Both the shapes of the ICA plots and the calculated ICQ (intensity correlation quotient; 0.036) are indicative for no colocalization of CDKN1A and γH2AX after X-irradiation. Panels b & c: Images of the separate channels as indicated for the same nucleus depicted in a. (D) CDKN1A (green) and PCNA (red) colocalize in G0/G1 AG1522C fibroblasts after exposure to 8 Gy X-rays. Panels a-c: Representative nucleus fixed and stained 3 h post exposure, as described previously [34]. Panel d: Relative fluorescence intensity profiles for 3 foci over a distance of 8.5 μm, as also depicted in the insert to panel c. Panel e: ICA plots for the CDKN1A and PCNA signals in the nucleus shown in a-c. The shapes of the ICA plots are indicative for colocalization of CDKN1A and PCNA (ICQ = 0.181). Blue: ToPro-3 staining of DNA.

Figure 2. CDKN1A accumulates into nuclear foci after H_2O_2 treatment. (A) Immunostaining of control (panels a-d) and of H_2O_2-treated (panels e-h) nuclei of quiescent normal human dermal fibroblasts. a & e: ToPro-3 staining of DNA; b & f: XRCC1 (red); c & g: CDKN1A (green). d & h: Superimposed images from the nuclei shown in panels a-c and e-g, respectively. (B) Exemplary colocalization analysis for CDKN1A and XRCC1 for the H_2O_2-treated nucleus shown on the right. Depicted are the ICA plots for the proteins as indicated and the superimposed images for the respective nucleus stained for CDKN1A (green), XRCC1 (red) and DNA (blue). Both the shape of the ICA plots and the calculated ICQ of 0.091 are indicative for no clear colocalization of CDKN1A and XRCC1 after H_2O_2 treatment.

Figure 3. CDKN1A focus formation after ionizing radiation is independent of nucleotide excision repair. (A) Nuclei of AG1522C (panels a, b, e & f) and XPA (panels c, d, g & h) cells exposed to 100 J/cm^2 UV light through microfilter-masks fixed at 30 min (panels a,

c, e and g) and 5 h (panels b, d, f and h) post exposure. Note: While recruitment of both PCNA and CDKN1A occurs as early as 30 min post UV light in AG1522C cells (panels a and e, respectively), recruitment of PCNA and CDKN1A is not observed after 30 min in XPA cells (panels c and g, respectively). Red: PI staining of DNA. Green: PCNA (panels a-d) and CDKN1A (panels e-h). (B) Recruitment of PCNA and CDKN1A occurs within 30 min after exposure to argon ions in both AG1522C (panels a and e, respectively) and XPA cells (panels c and g, respectively). CDKN1A foci resolve at 5 h after argon ion exposure in both AG1522C and XPA cells (panels f and h, respectively).

Figure 4. CDKN1A recruitment into foci after ionizing radiation is dependent on its ability to physically interact with PCNA. (A) Phosphomimetic CDKN1A-T145D is unable to interact with PCNA. Western blot analysis of anti-CDKN1A complexes from untransfected HeLa cells (NT), or from HeLa cell lysates generated after transfection with one of the three different CDKN1A expression constructs (wild-type, T145A mutant, or T145D mutant). Note: PCNA is not precipitated in anti-CDKN1A-T145D complexes (lane 3) demonstrating that non-phosphorylated T145 (lanes 2 and 4) confers the interaction with PCNA. (B) Immunostaining of nuclei from untransfected HeLa cells (panels a & b), or HeLa cells transfected to express wild type CDKN1A (panels c & d), CDKN1A-T145A (panels e & f) or CDKN1A-T145D (panels g & h). Mock-irradiated nuclei show few 53BP1 foci, but no CDKN1A foci (panels a, c, e & g). Nuclei form cells exposed to heavy ions show elevated levels of 53BP1 foci (panels b, d, f & h). Untransfected HeLa cells exposed to zinc ions do not show any CDKN1A foci (panel b), but HeLa cells expressing wild type CDKN1A or CDKN1A-T145A show relocalization of CDKN1A into foci 30 min post exposure to heavy ions (panels d and f, respectively). CDKN1A-T145D is not recruited into foci after exposure to gold ions (panel h), but remains homogenously dispersed throughout the nucleus. Green: CDKN1A. Red: 53BP1. Blue: ToPro-3 staining of DNA.

Figure 5. CDKN1A is de-phosphorylated in response to ionizing radiation and binds to the chromatin fraction after X-rays and after charged particle irradiation. (A) Autoradiograph obtained after first-dimension electrophoresis of anti-CDKN1A complexes from ^{32}P-orthophosphate labeled HeLa cells ectopically expressing wild type CDKN1A. (B) Results from second-dimension chromatography showing that CDKN1A phospho-peptide expression is abundant in mock-irradiated HeLa cells (upper panel). No

CDKN1A phospho-peptides are detected 2.5 h after exposure to 10 Gy X-rays (lower panel). (C) Representative Western blots to show dose-dependent association of PCNA with the chromatin fraction in quiescent AG1522C fibroblasts exposed to X-rays (compare signals for PCNA in lane 5 and 6). Fractionated extracts were prepared 3 h after irradiation. Lanes 1-3: soluble proteins, lanes 4-6: chromatin-bound proteins, lanes 7-9: DNA pellet and proteins not released by benzonase digest. (D) Representative Western blots to show that both PCNA and CDKN1A are localized to the chromatin fraction in quiescent AG1522C fibroblasts exposed to X-rays. A weak signal for chromatin bound CDKN1A at 1 h post 30 Gy X-rays (lane 5). At 3 h post 30 Gy X-rays the signal for chromatin-bound CDKN1A is significantly increased (lane 6). Note: soluble CDKN1A at 3 h post 30 Gy X-rays is slightly increased likely due to TP53-mediated transactivation of CDKN1A in response to radiation damage. Lanes 1-3: soluble proteins, lanes 4-6: chromatin-bound proteins. (E) Representative Western blots to show that PCNA and CDKN1A are localized to the chromatin fraction 1 h after exposure of quiescent AG1522C fibroblasts to chromium ions (lane 6). WCL: whole cell lysates prepared at 1h after exposure to IR. Lanes 2-3: soluble proteins, lanes 4-5: supernatants after 2 washes of the chromatin-bound protein pellet, lanes 6-7: chromatin-bound proteins released by benzonase treatment.

Figure 6. Dynamics of CDKN1A and PCNA recruitment after charged particle irradiation. (A) Recruitment kinetics of CDKN1A-EGFP and dsRed-tagged PCNA to DNA damage sites induced by uranium ions in living HeLa cells. Error bars present 95% confidence interval. Both proteins started to accumulate within few seconds after ion impact but CDKN1A appeared to be delayed compared to PCNA. The two datasets are in accordance to a simplified model based on sequential binding of the two proteins with PCNA binding being a prerequisite for CDKN1A accumulation (for model description see Material and Methods section). The fitted curves of the model (red and blue lines) yielded time constants k1* of 108 +/- 5 s for PCNA and k2* 92 +/- 4 s for the CDKN1A association step. (B) Recruitment kinetics of CDKN1A-EGFP is not depending on NER. Dynamics of accumulation of CDKN1A-EGFP to DNA damage in living wild type (AG1522C) and XPA deficient human GM00710B fibroblasts. Both cell lines showed very similar recruitment times after irradiation with Xenon ions demonstrating that CDKN1A recruitment occurred independently of NER after particle irradiation. Error bars present 95% confidence interval.

Figure 1

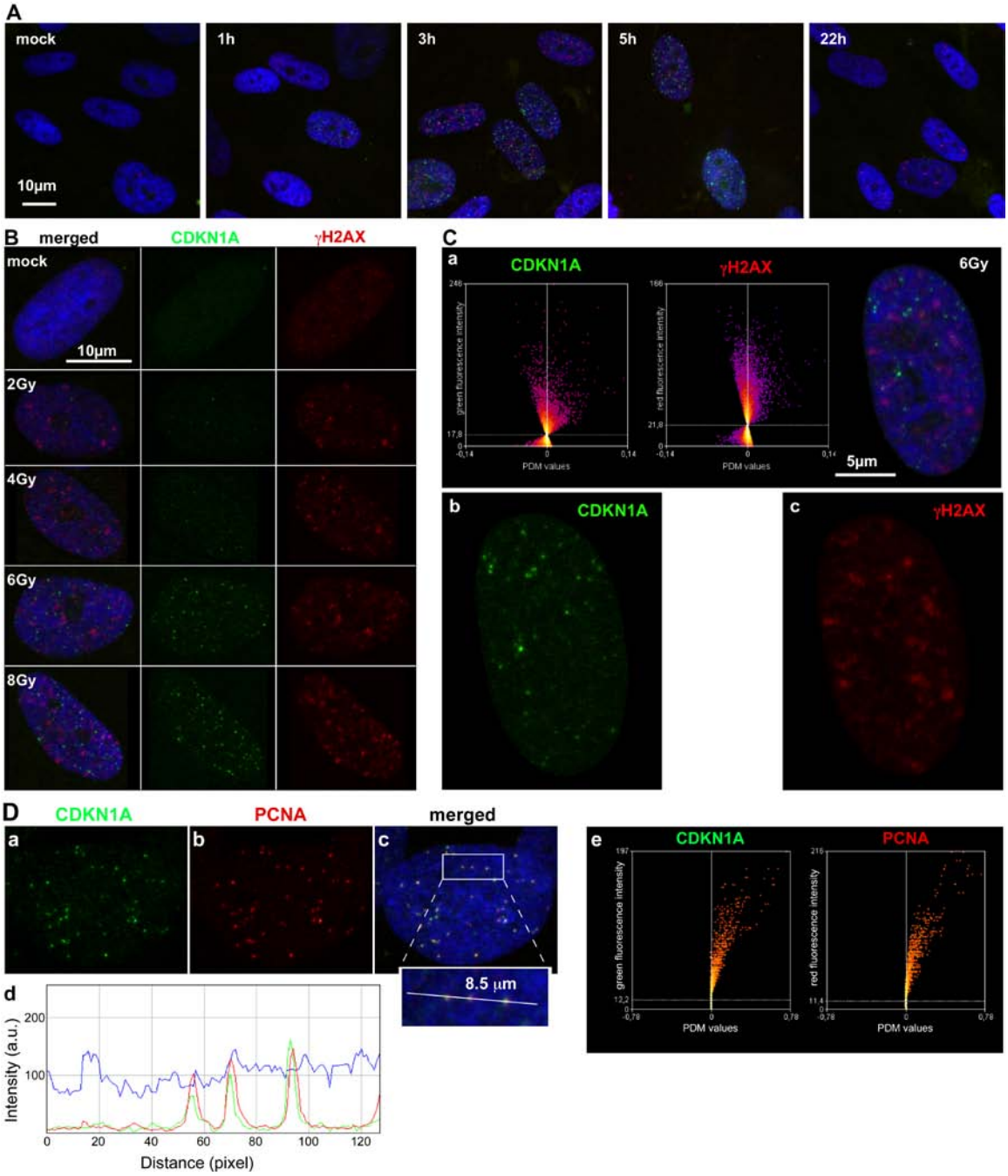
A
mock
1h
3h
5h
22h
10µm
B
merged
CDKN1A
γH2AX
mock
2Gy
4Gy
6Gy
8Gy
10µm
C
a
CDKN1A
γH2AX
6Gy
green fluorescence intensity
red fluorescence intensity
PDM values
5µm
b
CDKN1A
c
γH2AX
D
CDKN1A
PCNA
merged
a
b
c
8.5 µm
d
Intensity (a.u.)
Distance (pixel)
e
CDKN1A
PCNA
green fluorescence intensity
red fluorescence intensity
PDM values

Figure 2

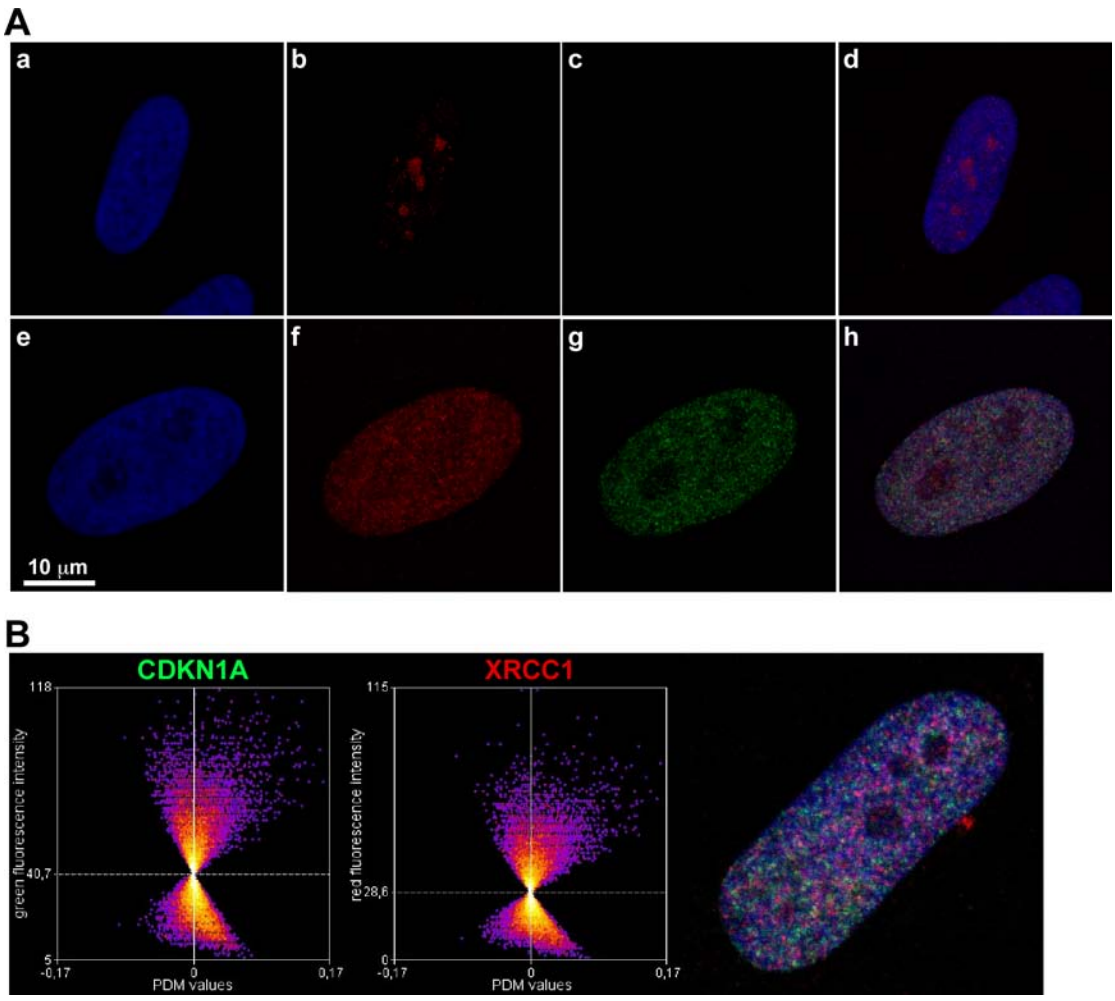
A
a
b
c
d
e
f
g
h
10 μm
B
CDKN1A
XRCC1
118
115
green fluorescence intensity
red fluorescence intensity
40,7
28,6
5
0
-0,17
0
0,17
PDM values
PDM values

Figure 3

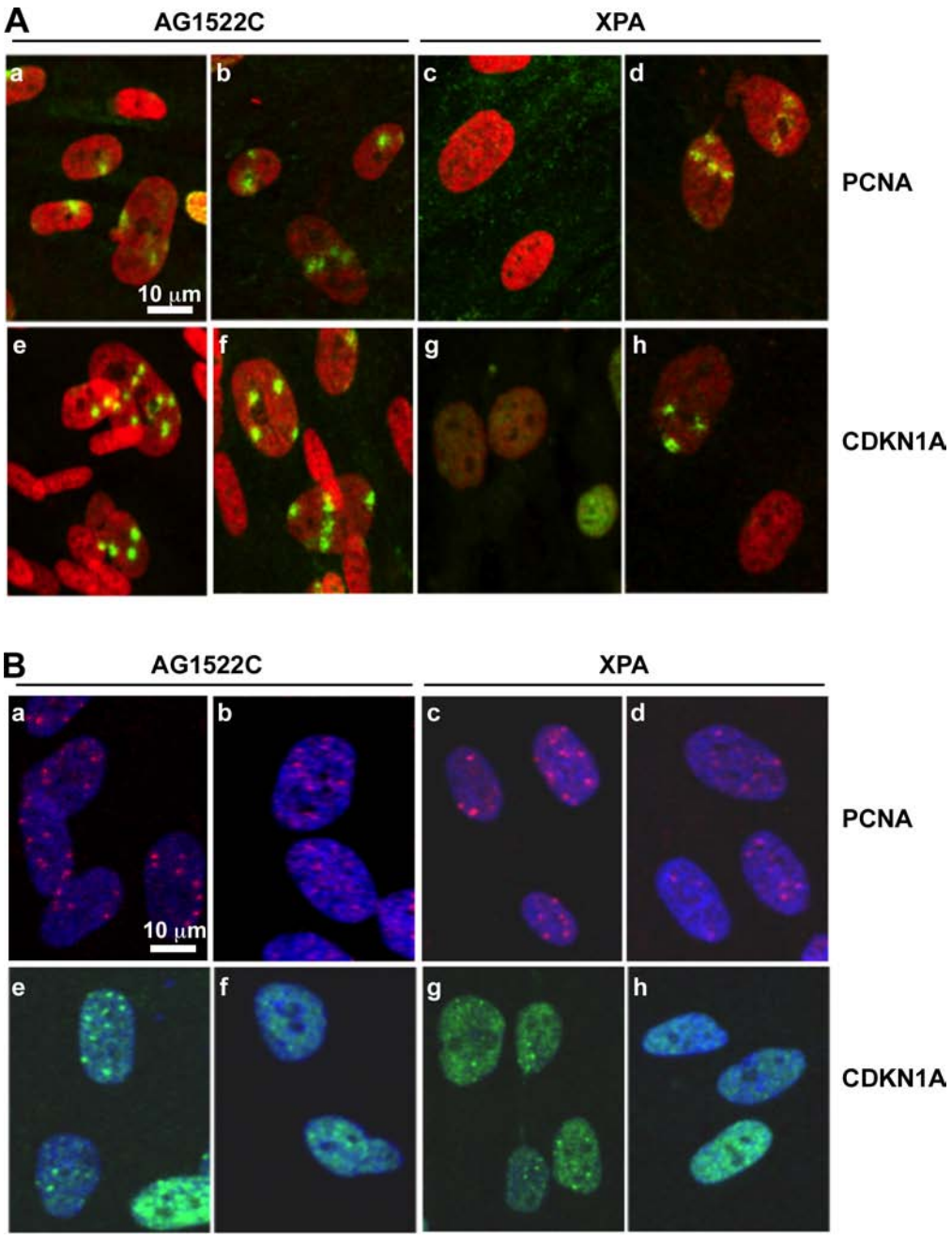
A
AG1522C
XPA
a
b
c
d
10 μm
PCNA
e
f
g
h
CDKN1A
B
AG1522C
XPA
a
b
c
d
10 μm
PCNA
e
f
g
h
CDKN1A

Figure 4

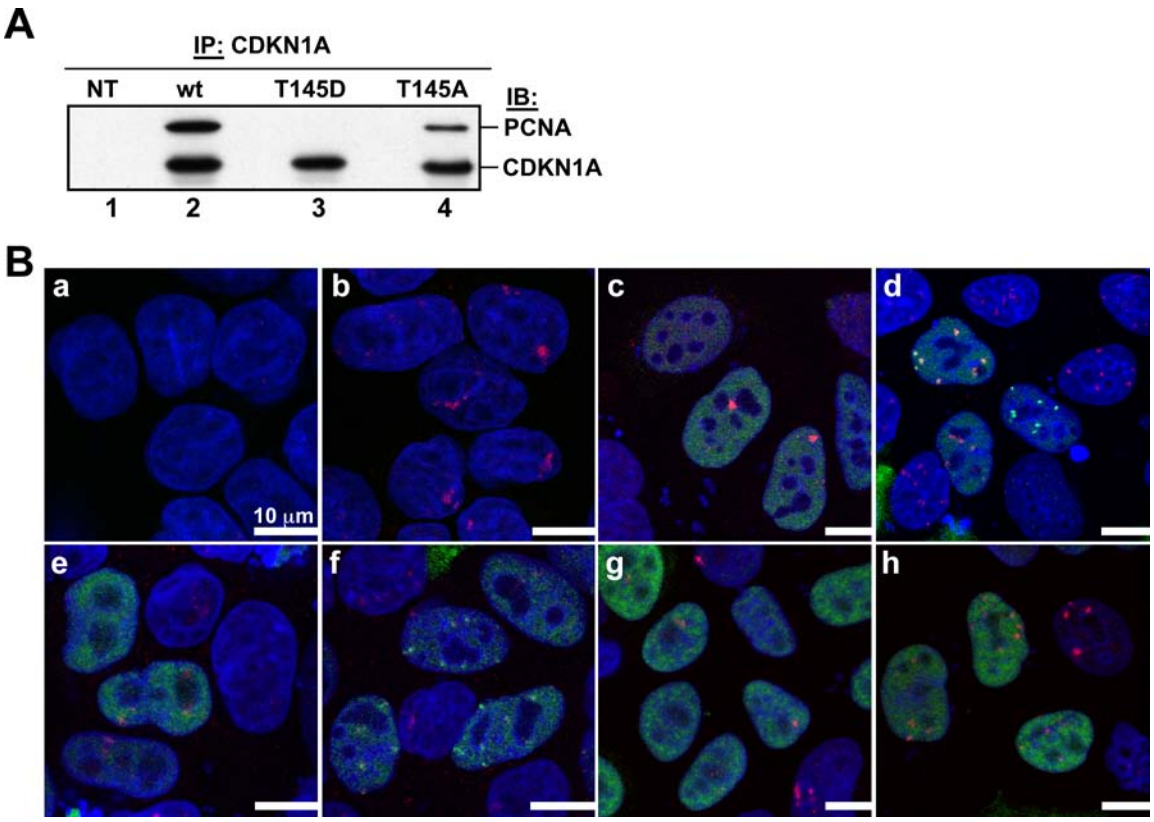
A
IP: CDKN1A
NT
wt
T145D
T145A
IB:
PCNA
CDKN1A
1
2
3
4
B
a
b
c
d
10 μm
e
f
g
h

Figure 5

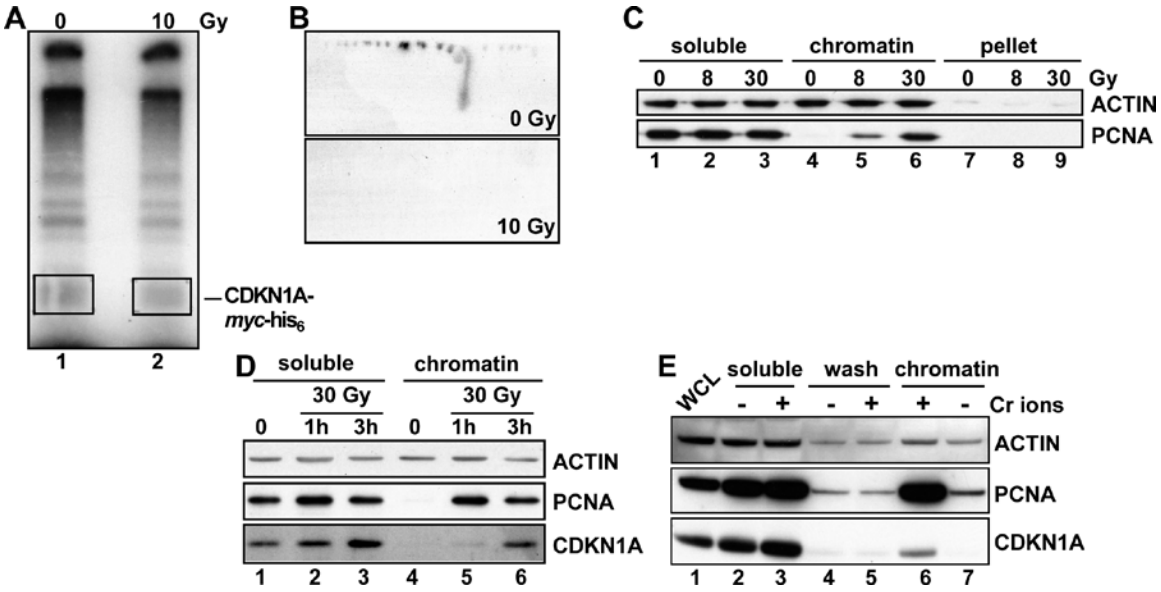

Figure 6